On the Spread of Microbes That Manipulate Reproduction in Marine Invertebrates

Matthew C. Kustra[1],* and **Tyler J. Carrier[2],***

1. Department of Ecology and Evolutionary Biology, University of California, Santa Cruz, California 95064;   2. GEOMAR Helmholtz Centre for Ocean Research, Kiel, Germany; and Zoological Institute, Kiel University, Kiel, Germany

ABSTRACT: Bacterial symbionts are functionally integral to animal reproduction and development, some of which have evolved additional mechanisms to override these host programs. One habitat that is increasingly recognized to contain phylogenetically related lineages of reproductive manipulators is the ocean. The reproduction of marine invertebrates often occurs by free spawning instead of by the physical contact of copulation in terrestrial systems. We developed an integrated model to understand whether and when microbes that manipulate host reproduction by cytoplasmic incompatibility, feminization, and male killing spread within populations of free-spawning marine invertebrates. Our model supports three primary findings. First, sex ratio distortion leads to suboptimal fertilization and zygote production in planktotrophs (feeding larvae) but enhance these processes in lecithotrophs (nonfeeding larvae). Second, feminization and a combination of male killing plus enhanced growth are effective at spreading reproductive manipulators while also inducing a female-biased sex ratio. Third, the majority of free-spawning marine invertebrates could be infected across a range of life history combinations, with infections harming species with smaller eggs and longer pelagic durations while benefiting species with larger eggs and shorter pelagic durations. Together, this supports the general premise that microbes may manipulate the reproduction of free-spawning marine invertebrates (e.g., by inducing changes in developmental life history) and that these types of manipulations overlap considerably with terrestrial systems.

Keywords: cytoplasmic incompatibility, feminization, fertilization, *Heliocidaris*, life history evolution, male killing.

Introduction

Bacterial symbionts are functionally integral to animal biology, including being central to cell and tissue differentiation, reproduction, and development (McFall-Ngai 2002; Bates et al. 2006; Bright and Bulgheresi 2010; Fraune and Bosch 2010; McFall-Ngai et al. 2013; Gilbert et al. 2015). Microbes that are functionally intertwined with animal development are often beneficial to the host (McFall-Ngai 2002; Gilbert et al. 2015; Bosch and McFall-Ngai 2021). Some of these bacteria, however, have evolved additional mechanisms to override components of the host's developmental program (Werren et al. 2008; Engelstädter and Hurst 2009*a*; Perlmutter and Bordenstein 2020). These microbes are often inherited through the cytoplasm of the egg and can manipulate host reproduction to favor their transmission through cytoplasmic incompatibility (where microbe-containing males are incompatible with aposymbiotic females), feminization (the conversion of genetic males to females), and male killing (microbe-induced male mortality during early or late development; Engelstädter and Hurst 2009*a*; Perlmutter and Bordenstein 2020; Kaur et al. 2021).

Hosts affected by microbes that manipulate reproduction are diverse and are particularly common in terrestrial nematodes and arthropods, where >60% of species are thought to be infected (Stevens et al. 2001; Duron et al. 2008; Hilgenboecker et al. 2008). The most widely recognized reproductive manipulator is *Wolbachia*, but bacteria within *Arsenophonus*, *Cardinium*, *Rickettsia*, and *Spiroplasma* can also interfere with host reproduction (Werren et al. 2008; Engelstädter and Hurst 2009*a*; Perlmutter and Bordenstein 2020). These manipulators live extracellularly, freely inside host cells, or within vacuoles, where they can use the host's cellular machinery to induce their respective phenotypes (Skinner 1985; Callaini et al. 1994; Hurst et al. 1996; Ammar and Hogenhout 2006; Kitajima et al. 2007; Werren et al. 2008; Engelstädter and Hurst 2009*a*).

While much is known about these symbioses in terrestrial systems, the ocean is increasingly recognized to be home to microbes that are phylogenetically related to terrestrial reproductive manipulators (Morris et al. 2002; Perlman et al.

* Corresponding authors; email: mkustra@ucsc.edu, tcarrier@geomar.de.
  ORCIDs: Kustra, https://orcid.org/0000-0002-1144-7030; Carrier, https://orcid.org/0000-0001-7885-184X.

2006; Sunagawa et al. 2015; Harumoto and Lemaitre 2018). Dozens of marine invertebrate lineages have been found to associate with Rickettsiales, and some are believed to interfere with host reproduction (Klinges et al. 2019; Carrier et al. 2021). Marine invertebrates often reproduce by free spawning their gametes into the water column, where fertilization, embryogenesis, and larval development take place (Thorson 1950; Mileikovsky 1971; Levitan 1995). This is in contrast to terrestrial arthropods that reproduce by the direct physical contact of copulation (Engelmann 2015). Despite these vastly different life history tendencies (Strathmann 1990), the fitness of marine reproductive manipulators remains dependent on their transmission across generations. We therefore hypothesize that population-level consequences of microbe-mediated reproductive manipulations should be convergent between terrestrial and marine animal hosts (Engelstädter and Hurst 2009a; Burgess et al. 2015).

One such marine animal host is *Heliocidaris*, a genus of sea urchin that includes one of the most comprehensively studied transitions between the major developmental strategies among marine invertebrates (Thorson 1950; Strathmann 1985; Wray and Raff 1989; Wray and Raff 1991b; Byrne et al. 1999; Israel et al. 2016). A speciation event ~5 million years ago resulted in sister species with alternative life history strategies: *H. tuberculata* is planktotrophic, while *H. erythrogramma* is lecithotrophic (Wray and Raff 1991a; Zigler et al. 2003). Typical of planktotrophs, *H. tuberculata* develops from small eggs ($<$100 μm in diameter) into feeding larvae that disperse for several weeks, while *H. erythrogramma* develops from eggs ~53 to 86 times the volume of *H. tuberculata* eggs into nonfeeding larvae that lack the morphological structures for feeding and remain in the water column for 5 days (Emlet and Hoegh-Guldberg 1997; Wray and Raff 1991a).

The lecithotrophic *H. erythrogramma* acquired a cytoplasmically inherited Rickettsiales—*Echinorickettsia raffii*—in this life history switch that is most closely related to *Wolbachia pipientis* wMel and wAlbB (Carrier et al. 2021). The genome of *E. raffii* suggests that this bacterium is a nutritional mutualist and a reproductive manipulator (Carrier et al. 2021). In the former, the host is hypothesized to benefit from being provisioned essential amino acids to enhance growth, as observed in terrestrial systems (Douglas 1998; Hosokawa et al. 2010). In the latter, this bacterium is hypothesized to use effector proteins to influence the rate of male mortality and modulate fertilization (Carrier et al. 2021). Supporting the hypothesis that *E. raffii* manipulates host reproduction, populations of *H. erythrogramma* in Sydney Harbor (67.2%) and Tasmania (56.9%) are disproportionately female (Dix 1977; Carrier et al. 2021). Moreover, the youngest reproductive individuals in Sydney Harbor do not deviate from a 1:1 female-to-male ratio, while the largest individuals have a 4:1 female-to-male ratio (Carrier et al. 2021). There is currently no evidence that *E. raffii* associates with the planktotrophic *H. tuberculata*, indicating potential differences in whether and how reproductive manipulators may spread in these developmental life history strategies.

Understanding whether microbes that manipulate reproduction can spread and induce shifts in the population structure of marine invertebrates requires the integration of two model types. The first concerns the fertilization dynamics and zygote production of free-spawning marine invertebrates (e.g., Levitan 1991, 1993, 2004; Styan 1998), and the second involves the spread and population-level consequences of cytoplasmic incompatibility, feminization, and male killing (e.g., Jansen et al. 2008; Engelstädter and Hurst 2009b; Hancock et al. 2011). Accounting for the difference in reproductive strategy between terrestrial arthropods and free-spawning marine invertebrates allows us to estimate how sex ratio distortion influences reproductive success and the likely type(s) of manipulations that occur in the sea. We first apply this general integrated model to *Heliocidaris*. We then develop a size-structured population model to test how a reproductive manipulator could induce a female-biased sex ratio, as is observed in *H. erythrogramma* (Carrier et al. 2021). Last, we develop a general model to assess when infections occur based on key components of marine invertebrate life history, limitations to such infections, and which phyla and developmental modes are particularly infectable.

Methods

Fertilization Dynamics in Free-Spawning Marine Invertebrates

Fertilization success of free-spawning marine invertebrates is highly variable and is based on many ecological factors, resulting in the possibility for eggs within a clutch to experience both sperm limitation and polyspermy (Levitan 1995; Styan 1998; Evans and Lymbery 2020). Various gamete characteristics (e.g., egg size and sperm velocity) as well as ambient egg and sperm concentrations can be used to determine the likelihood that sperm limitation or polyspermy occur. To understand how spawning density and sex ratio may influence fertilization success and zygote production, we modified the Styan (1998) polyspermy kinetic model by converting total egg (E_T; egg/μL) and sperm (S_T; sperm/μL) concentrations to be explicitly determined by female and male density.

The average number of sperm that may potentially fertilize an egg during a free-spawning event, x (eq. [5] from Styan 1998), is a function of fertilization efficiency (F_e), total sperm concentration (S_T; sperm/μL), total egg concentration

(E_T; egg/μL), the biomolecular collision constant (β_0; mm³/s), and the sperm half-life (τ; s):

$$x = F_e \frac{S_T}{E_T}(1 - e^{-\beta_0 E_T \tau}). \qquad (1)$$

Moreover, the biomolecular collision constant (β_0) is determined by the cross-sectional area of the egg (σ; mm²) and sperm velocity (ν; mm/s; eq. [2] from Styan 1998):

$$\beta_0 = \sigma\nu. \qquad (2)$$

The biomolecular collision constant and the time to elicit a block to polyspermy (t_b; s) may then be used to calculate the average number of extra sperm that may contact an already fertilized egg, which then results in polyspermy (b; eq. [13] from Styan 1998):

$$b = F_e \frac{S_T}{E_T}(1 - e^{-\beta_0 E_T t_b}). \qquad (3)$$

The proportion of eggs that will be fertilized by a single sperm and successfully develop may be estimated by the following (eq. [16] from Styan 1998):

$$p(\text{monospermic zygote}) = 1 - e^{-x}$$
$$- (1 - e^{-x} - xe^{-x})(1 - e^{-b}). \qquad (4)$$

Zygote density ($N_{z,t}$; zygotes/μL) may then be estimated on the basis of the probability of a monospermic zygote (eq. [4]) and total egg density (E_T):

$$N_{z,t} = p(\text{monospermic zygote})E_T. \qquad (5)$$

A summary of the variables and parameters used in this fertilization model are presented in table 1. Equations (4) and (5) are available in the web application at https://mck8dg.shinyapps.io/SI_sex_ratio_distortion_marine_inverts/, where the various reproductive parameters may be altered to explore how reproductive output is influenced.

Spread of Reproductive Manipulators: No Population Structure

We developed a population model without size structure that integrated the fertilization model described above to simulate how a microbe that manipulates reproduction via either cytoplasmic incompatibility, feminization, or male killing may spread within a population of free-spawning marine invertebrates. Each scenario had four distinct groups: uninfected females ($N_{u,f}$; individuals/m²), infected females ($N_{i,f}$; individuals/m²), uninfected males ($N_{u,m}$; individuals/m²), and infected males ($N_{i,m,t}$; individuals/m²). We used a discrete time population model with overlapping generations—where reproduction, larval development, and adult mortality are assumed to occur in that order—because ma-

rine invertebrates tend to spawn seasonally (e.g., Giese 1959; Mileikovsky 1971; Strathmann 1987).

Larval mortality (M_z) is assumed to be dependent on the length of the larval period and the instantaneous mortality rate (m_z), which we assumed to be constant between generations and density independent (Morgan 1995; Rumrill 1990):

$$M_z = 1 - e^{-m_z t_d}. \qquad (6)$$

Adult mortality (M_a), on the other hand, is assumed to be density dependent and based on the maximum adult mortality rate (m_a), carrying capacity (k; individuals/m²), total density of the population at time t (N_t; individuals/m²), and the degree to which density influences mortality (i.e., the shape parameter; d). Moreover, both the current adult density and density of surviving zygotes that settled were assumed to influence density dependence, where $N'_{z,t}$ is the density of zygotes (zygotes/μL) that survived after microbe-induced mortality (i.e., during cytoplasmic incompatibility or male killing) has occurred and ψ (μL/m²) is the settlement constant that describes the proportion of surviving zygotes that settled:

$$M_a = \left(\frac{m_a}{1 + e^{-d(N_t + N'_{z,t}(1 - M_z)\psi - (k/2))}}\right). \qquad (7)$$

The density of uninfected females in the next generation ($N_{u,f,t+1}$; individuals/m²) may then be determined by the density of surviving uninfected female zygotes ($N_{z,u,f,t}$; zygotes/μL) that settled plus the density of surviving uninfected female adults at generation t ($N_{u,f,t}$; individuals/m²):

$$N_{u,f,t+1} = (N_{z,u,f,t}(1 - M_z)\psi + N_{u,f,t})(1 - M_a). \qquad (8)$$

The density of uninfected female zygotes ($N_{z,u,f,t}$) is directly influenced by cytoplasmic incompatibility—but not male killing or feminization—and is calculated by multiplying the number of zygotes ($N_{z,t}$) by the proportion of eggs from uninfected adult females, where c is the fecundity cost to infected females. We assumed that uninfected females produced an equal number of daughters and sons, and therefore the density of zygotes ($N_{z,t}$) is divided by two. If cytoplasmic incompatibility occurs, then the density of surviving zygotes is also dependent on the proportion of sperm from infected males and the cytoplasmic incompatibility mortality rate (m_c). Note that both the slope of eggs (E; eggs/μL/individual/m²) and the slope of sperm density (S; sperm/μL/individual/m²) cancel out in this equation:

$$N_{z,u,f,t} = N_{z,t}\left(\frac{N_{u,f,t}}{2(N_{u,f,t} + N_{i,f,t}(1 - c))}\right)$$
$$\times \left(\frac{N_{u,m,t} + N_{i,m,t}(1 - m_c)}{N_{u,m,t} + N_{i,m,t}}\right). \qquad (9)$$

Table 1: Definitions and values of parameters for fertilization dynamics adapted from Styan (1998)

Symbol	Definition	*Heliocidaris erythrogramma*	*Heliocidaris tuberculata*	Other
σ	Cross-sectional area of egg (mm^2)	.203[a]	.017[a]	.04–1.5[b] (.01)
ν	Sperm swimming speed (mm/s)	.125[c]	.140[a]	.125[c]
E	Egg density per unit female density (eggs/μL/individual/m^2)	.05[d]	66.59[e]	1.13[f]/σ
S	Sperm density per unit male density (sperm/μL/individual/m^2)	...	700[d]	...
F_e	Fertilization efficiency	...	.094[g]	...
τ	Sperm half-life (s)	...	5,400[h]	...
t_b	Time for polyspermy block (s)	...	1[i]	...
β_0	Biomolecular collision constant (mm^3/s)	...	$\sigma\nu$	...
x	Average number of potential fertilizing sperm	...	Eq. (1)	...
b	Average number of extra fertilizing sperm that contacts an egg	...	Eq. (3)	...

Note: The "Other" column refers to values used/fixed for the parameter analysis; numbers in parentheses indicate the step size in sensitivity analyses.

[a] Foo et al. 2018.

[b] These values are of egg diameter (mm) and were converted to cross-sectional area of egg (mm^2) during the analysis.

[c] Fitzpatrick et al. 2010.

[d] Evans and Marshall 2005.

[e] O'Conner and Mulley 1977.

[f] This value was calculated by multiplying egg density and egg size of *H. tuberculata* to keep the overall fecundity for different egg sizes the same.

[g] M. Byrne, unpublished data.

[h] Binet and Doyle 2013.

[i] Longo et al. 1986.

The density of uninfected males in the next generation ($N_{u,m,t+1}$; individuals/m^2) has the same general recursion equation (i.e., eq. [8]), and the density of uninfected male zygotes ($N_{z,u,m,t}$; zygotes/μL) is the same as the density of uninfected female zygotes ($N_{z,u,f,t}$) in equation (9).

Since all groups in this model have the same general recursion equations, the density of infected females in the next generation ($N_{i,f,t+1}$; individuals/m^2) has the same basic structure as equation (8). The density of infected female zygotes ($N_{z,i,f,t}$; zygotes/μL), however, is unaffected by either cytoplasmic incompatibility or male killing and is only directly affected by the feminization rate. The density of infected female zygotes is calculated by multiplying the density of zygotes ($N_{z,t}$) by the proportion of infected adult females and the sex ratio biasing constant (r), which ranges from 0.5 (no sex ratio distortion) to 1.0 (complete feminization):

$$N_{z,i,f,t} = N_{z,t}\left(\frac{rN_{i,f,t}(1-c)}{N_{u,f,t} + N_{i,f,t}(1-c)}\right). \quad (10)$$

The density of infected males in the next generation ($N_{i,m,t+1}$; individuals/m^2) also has the same basic structure as equation (8). The density of infected male zygotes ($N_{z,i,m,t}$;

zygotes/μL) is influenced by both feminization and male killing, but not cytoplasmic incompatibility. The density of infected male zygotes has the same basic structure as equation (10), except that the complement of the sex ratio biasing constant (r) is used while also accounting for mortality due to male killing (m_k):

$$N_{z,i,m,t} = N_{z,t}\left(\frac{(1-r)N_{i,f,t}(1-c)}{N_{u,f,t} + N_{i,f,t}(1-c)}\right)(1-m_k). \quad (11)$$

A summary of the variables and parameters are provided in table 2, and a diagram of this model is outlined in figure S1.

A Case Study Simulation: Heliocidaris without Population Structure

We apply our model to *Heliocidaris* for three main reasons. First, populations of *H. erythrogramma* associate with an endosymbiont that is hypothesized to distort host sex ratio, and this is the only marine invertebrate known to have this type of partnership (Carrier et al. 2021). Second, these two *Heliocidaris* species are representative of the primary

Table 2: Definitions and values of parameters for non-stage-based population dynamics model

Symbol	Definition	Value(s)	
		Species models	Other analyses
Parameters:			
k	Adult carrying capacity (individuals/m^2)	100	
ψ	Settlement constant (μL/m^2)	1	
d	Mortality rate of change	.10	
m_a	Max adult mortality	.99	
m_z	Instantaneous mortality rate	.23	
m_c	Cytoplasmic incompatibility mortality rate	.70	NA
r	Sex ratio biasing constant	.70	.5–1 (.001)
m_k	Male killing rate	.70	NA
c	Cost in terms of percent fecundity reduction	0	0–.6 (.001)
Functions:			
M_a	Adult mortality	Eq. (7)	
M_z	Larval mortality	Eq. (6)	
Variables:			
N_t	Density of all adult individuals at time t	2	
$N_{f,t}$	Density of all adult females at time t	1	
$N_{i,f,t}$	Density of infected adult females at time t	.01	
$N_{u,f,t}$	Density of uninfected adult females at time t	.99	
$N_{m,t}$	Density of all males at time t	1	
$N_{i,m,t}$	Density of infected adult males at time t	.01	
$N_{u,m,t}$	Density of uninfected adult males at time t	.99	
$N_{z,t}$	Density of initial zygotes at time t	NA	
$N'_{z,t}$	Density of zygotes at time t after male killing and cytoplasmic incompatibility	NA	
$N_{z,i,f,t}$	Density of infected female zygotes at time t	NA	
$N_{z,u,f,t}$	Density of uninfected female zygotes at time t	NA	
$N_{z,i,m,t}$	Density of infected male zygotes at time t	NA	
$N_{z,u,m,t}$	Density of uninfected male zygotes at time t	NA	

Note: Capital letters are functions or variables, and initial values are given when available. Zygote density units are zygotes per microliter, and adult density units are individuals per square meter. Numbers in parentheses indicate step size in sensitivity analyses. NA = not applicable.

developmental strategies of marine invertebrates and are very well studied, allowing us to apply species-specific values for most parameters of our model (Thorson 1950; Strathmann 1985). When species-specific parameters were unavailable, we parametrized with values from related echinoids (table 1). Finally, these species differ vastly in egg and clutch size, allowing for a broader understanding of how host reproductive biology influences the spread of microbes that manipulates the reproduction of free-spawning marine invertebrates.

Using the model described above, we simulated whether a reproductive manipulator could invade a population with each developmental life history when introduced (at 1%) using the three modes of reproductive manipulation described above in isolation. First, to model cytoplasmic incompatibility in isolation, m_c was set to 0.7, m_k was set to 0, and r was set to 0.5. Second, for feminization, m_c and m_k were set to 0 and r was set to 0.7. Last, for male killing, m_c was set to 0, m_k was set to 0.7, and r was set to 0.5. Pre-

liminary analyses varying these values resulted in qualitatively similar results (web application at https://mck8dg .shinyapps.io/SI_sex_ratio_distortion_marine_inverts/).

A Case Study Simulation: Heliocidaris with Population Structure

We then developed a stage-based population model to determine whether and how characteristics of a reproductive manipulator (i.e., as a nutritional mutualist and reproductive manipulator) may influence the population biology and structure of *H. erythrogramma*. In this, we simulated the infection and spread of a reproductive manipulator in three size classes (adult diameters of 20–39 mm, 40–59 mm, and ≥60 mm), both sexes, and uninfected and infected individuals (table 3). These size classes were chosen because they represent the naturally occurring size distribution of reproductive *H. erythrogramma* (Williams and

Table 3: Definitions and values of parameters and variables for the stage-based population dynamics model

Symbol	Definition	Value
Parameters:		
g_i	Transition rate for infected females	.25
g	Transition rate for other individuals	.10
d_1	Deduction in fecundity for 20–39-mm size class	.24[a]
d_2	Deduction in fecundity for 40–59-mm size class	.75[a]
Variables:		
$N_{i,m,1,t}$	Density of infected males of 20–39-mm size class at time t	.01
$N_{u,m,1,t}$	Density of uninfected males of 20–39-mm size class at time t	.99
$N_{i,f,1,t}$	Density of infected females of 20–39-mm size class at time t	.01
$N_{u,f,1,t}$	Density of uninfected females of 20–39-mm size class at time t	.99
$N_{i,m,2,t}$	Density of infected males of 40–59-mm size class at time t	0
$N_{u,m,2,t}$	Density of uninfected males of 40–59-mm size class at time t	0
$N_{i,f,2,t}$	Density of infected females of 40–59-mm size class at time t	0
$N_{u,f,2,t}$	Density of uninfected females of 40–59-mm size class at time t	0
$N_{i,m,3,t}$	Density of infected males of ≥60-mm size class at time t	0
$N_{u,m,3,t}$	Density of uninfected males of ≥60-mm size class at time t	0
$N_{i,f,3,t}$	Density of infected females of ≥60-mm size class at time t	0
$N_{u,f,3,t}$	Density of uninfected females of ≥60-mm size class at time t	0

Note: Parameters and variables that are shared with the basic model are not included in this table but are in tables 1 and 2. The units for all density variables are individuals per square meter. Initial values for variables are given.

[a] Calculated from equation (12) (eq. [2] in Levitan 1991).

Anderson 1975; Dix 1977; Laegdsgaard et al. 1991; Ling et al. 2019; Carrier et al. 2021). We also performed this simulation in *H. tuberculata* as a proof of concept.

This stage-based population model had three phases: birth, death, and transitions to the next size class. Birth followed the same fertilization dynamics described by equation (5), where the total egg (E_t; eggs/μL) and sperm (S_t; sperm/μL) concentration were determined by summing the number of each group that contributed to a successful fertilization. We assumed that the largest individuals (>60 mm) produced the same number of gametes as the species-specific parameters used for the model without population structure (table 1). Individuals in the 20–39-mm and 40–59-mm size classes produced a fraction of the gametes of the largest individuals (d_1 and d_2, respectively) that is based on the size-fecundity relationship described in equation (2) in Levitan (1991):

$$\log \text{ volume of eggs (mL)} = 3.56 \log \text{ size (mm)} - 6.59. \quad (12)$$

We used median diameters for each size class (i.e., 30 mm, 50 mm, and 60 mm) in this equation, and all other reproductive parameters were assumed to not differ between size.

The density of eggs of a given infection status (E_g; eggs/μL) is determined by the density of females (individuals/m^2) in the different size classes for a given infection status (indicated by the subscript g) weighted by their respective size class contributions (d_1 and d_2) multiplied by the egg concentration slope E (eggs/μL/individual/m^2):

$$E_{g,t} = E(N_{g,f,1,t}d_1 + N_{g,f,2,t}d_2 + N_{g,f,3,t}). \quad (13)$$

Moreover, the density of sperm of a given infection status (S_g; sperm/μL) has the same basic structure as equation (13) except that it uses the sperm concentration slope S (sperm/μL/individual/m^2):

$$S_{g,t} = S(N_{g,m,1,t}d_1 + N_{g,m,2,t}d_2 + N_{g,m,3,t}). \quad (14)$$

The density of uninfected female zygotes ($N_{z,u,f,t}$; zygotes/μL) is directly influenced by cytoplasmic incompatibility—but not male killing—and is calculated by multiplying the number of zygotes ($N_{z,t}$; zygotes/μL) by the proportion of uninfected female eggs. We assumed that uninfected females will produce equal daughters and sons, and therefore the number of zygotes ($N_{z,t}$) is divided by two. If cytoplasmic incompatibility occurs, then the density of surviving zygotes is also dependent on the cytoplasmic incompatibility mortality rate (m_c) and the proportion of infected adult male sperm:

$$N_{z,u,f,t} = N_{z,t}\left(\frac{E_{u,t}}{2(E_{u,t} + E_{i,t})}\right)\left(\frac{S_{u,t} + S_{i,t}(1 - m_c)}{S_{u,t} + S_{i,t}}\right). \quad (15)$$

Furthermore, the density of uninfected male zygotes ($N_{z,u,m,t}$; zygotes/μL) has the same basic structure as the density of uninfected female zygotes ($N_{z,u,f,t}$).

The density of infected female zygotes ($N_{z,i,f,t}$; zygotes/μL) is calculated by multiplying the number of zygotes ($N_{z,t}$) by the proportion of infected female eggs. We also assumed equal sex ratios at birth:

$$N_{z,i,f,t} = N_{z,t}\left(\frac{E_{i,t}}{2(E_{u,t} + E_{i,t})}\right). \qquad (16)$$

The density of infected male zygotes ($N_{z,i,m,t}$; zygotes/μL) is directly influenced by male killing and has the same basic structure as equation (16) except that mortality due to male killing (m_k) is accounted for:

$$N_{z,i,m,t} = N_{z,t}\left(\frac{E_{i,t}}{2(E_{u,t} + E_{i,t})}\right)(1 - m_k). \qquad (17)$$

Surviving zygotes that settle enter the smallest size class, given their respective sex and infection status, indicated by the subscript group index, g. The density of 20–39-mm individuals in a given group (sex and infection status) in the next time step ($N_{g,1,t+1}$; individuals/m^2) is determined by the density of surviving adults of a given group ($N_{g,1,t}$; individuals/m^2) that did not transition plus the density of surviving zygotes of a given group ($N_{z,g,t}$; zygotes/μL) that settled, where M_z is the larval mortality (eq. [6]), ψ is the settlement constant (μL/m^2), M_a is the adult mortality (eq. [7]), and g is the transition rate to the next size class:

$$N_{g,1,t+1} = (N_{z,g,t}(1 - M_z)\psi + N_{g,1,t}(1 - g))(1 - M_a). \qquad (18)$$

The density of 40–59-mm individuals in a given group (sex and infection status) in the next time step ($N_{g,2,t+1}$; individuals/m^2) is determined by the density of surviving 20–39-mm stage class adults of a given group ($N_{g,1,t}$; individuals/m^2) that transition and the density of surviving 40–59-mm adults of a given group ($N_{g,2,t}$; individuals/m^2) that do not transition to the next size class:

$$N_{g,2,t+1} = (N_{g,1,t}g + N_{g,2,t}(1 - g))(1 - M_a). \qquad (19)$$

The density of $\geq$60-mm individuals in a given group (sex and infection status) in the next time step ($N_{g,3,t+1}$; individuals/m^2) is determined by the density of surviving 39–40-mm stage class adults of a given group ($N_{g,2,t}$; individuals/m^2) that transition and the density of surviving $\geq$60-mm adults of a given group ($N_{g,3,t}$; individuals/m^2):

$$N_{g,3,t+1} = (N_{g,2,t}g + N_{g,3,t})(1 - M_a). \qquad (20)$$

To model enhanced growth rate in each size class of infected females, g is replaced with g_i such that $g_i > g$.

We numerically simulated this stage-based model using species-specific parameters of both *Heliocidaris* species for three different scenarios: (i) enhanced growth for infected females only ($g_i = 0.25$, $g = 0.1$, $m_k = 0$, $m_c = 0$), (ii) enhanced growth for infected females plus male killing ($g_i = 0.25$, $g = 0.1$, $m_k = 0.7$, $m_c = 0$), and (iii) enhanced growth for infected females plus male killing and cytoplasmic incompatibility ($g_i = 0.25$, $g = 0.1$, $m_k = 0.7$, $m_c = 0.7$). As a sensitivity analysis on how enhanced growth and male killing parameters influenced model outcomes, we simulated the model at all possible combinations of male-killing rate from 0 to 0.99 at increments of 0.01 and enhanced growth from 0.11 to 0.35 at increments of 0.01.

Summary of the variables and parameters used in this model are in tables 1–3, and a diagram of this model is outlined in figure S2. All simulations were performed using the deSolve package in R (Soetaert et al. 2010), and this may be simulated independently using the web application at https://mck8dg.shinyapps.io/SI_sex_ratio_distortion _marine_inverts/.

Numerical Analyses of Reproductive Manipulators and Life History Traits

The *Heliocidaris* species used in this case study are broadly representative of the two major developmental strategies of free-spawning marine invertebrates. They do not, however, fully encapsulate the enormous variety of life history combinations found in the sea (Levin and Bridges 1995; Byrne 2006; Allen and Pernet 2007). We complemented our *Heliocidaris* case study (with no population structure) by performing numerical simulations that vary egg size (σ), pelagic larval duration (t_d), and the cost of infection (c) to estimate which life history combinations may be infected by microbes that manipulate reproduction. We focus this analysis on feminization and male killing plus enhanced growth because our *Heliocidaris* case study indicated that these are the most likely types of reproductive manipulation for free-spawning marine invertebrates. We used the model without population structure because we were concerned with the assumptions needed to generalize the size classes of the population structure model across all of the given life history combinations. To model enhanced growth in the model without population structure, we made the cost of infection (c) negative for females associated with the microbe (i.e., infection increases fecundity).

To determine which life history characters influence host infectability, we simulated population runs at different combinations of egg diameter (from 40 to 1,500 μm with 10-μm increments) and pelagic larval duration (from 0 to 80 days with 1-day increments). The range of these parameters spans much of the diversity known in free-spawning marine invertebrates (Marshall et al. 2012; Álvarez-Noriega et al. 2020). We initialized populations at an equal
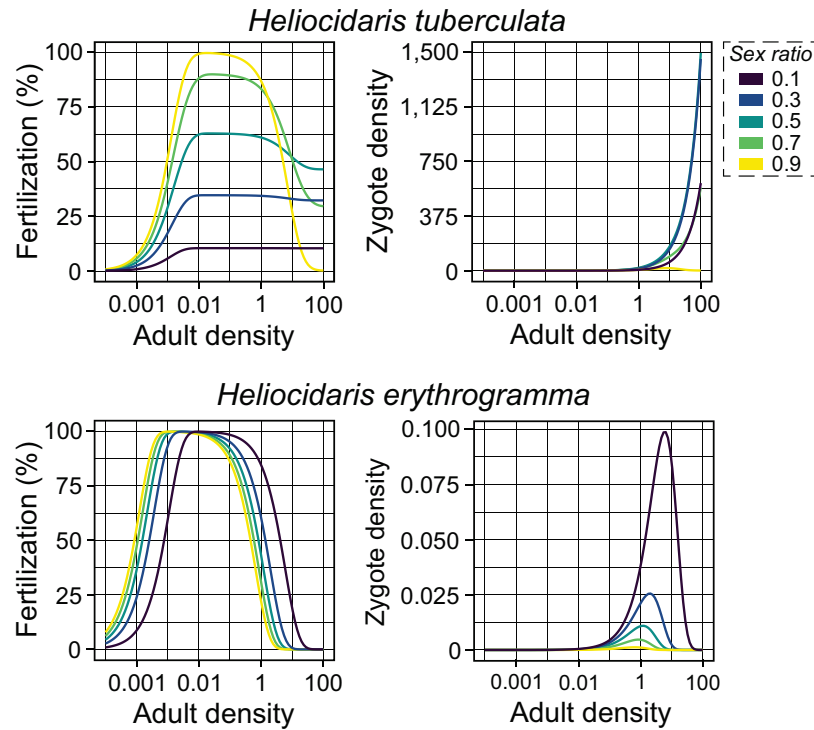
Figure 1: Modeled fertilization dynamics for two species of free-spawning marine invertebrates with alternative life history strategies. Shown are fertilization percentage (proportion of eggs fertilized by only one sperm; *left*) and zygote density (zygotes per microliter produced in a spawning event; *right*) for the planktotrophic *Heliocidaris tuberculata* (*top*) and lecithotrophic *H. erythrogramma* (*bottom*), based on adult density from 0.0001 to 100 individuals/m² and sex ratio from 0.1 (female biased) to 0.9 (male biased), with 0.5 being a balanced population. Equations (4) and (5) were adopted from the Styan (1998) polyspermy model and were used to generate these graphs, with species-specific parameters from the literature (table 1). These reproductive parameters can be altered to generate additional species-specific curves using the web application at https://mck8dg.shinyapps.io/SI_sex_ratio_distortion_marine_inverts/.

sex ratio with a total density of two individuals per square meter and an infection rate of 1%. We simulated populations until equilibrium was reached and set a maximum of time steps to 100,000 to account for the cycles that could happen in discrete time logistic population models (May 1974). At equilibrium we recorded the infection rate, density, sex ratio, and the time it took to reach that equilibrium. To determine which life history combinations would result in a host benefiting or being harmed by a reproductive manipulator, we compared equilibrium density in infected populations to that in stable uninfected populations.

We overlaid these numerical analyses with the life history data for species where both egg size and the pelagic larval duration are known (Marshall et al. 2012; Álvarez-Noriega et al. 2020). We then performed separate logistic regressions (generalized linear model with a binomial family and log link) to test whether infectability was associated with host phylum (Annelida, Echinodermata, and Mollusca), developmental mode (planktotrophy and lecithotrophy), and their interaction. We excluded Cnidaria ($n = 4$) and

Chordata ($n = 1$) from our logistic regressions because of their small sample size. We then performed a likelihood ratio test using a type II analysis of variance, with P values less than .05 considered to indicate statistical significance.

To test how developmental mode influenced the effect of infection on population density, we first calculated the $\log_2$ fold change of equilibrium density from uninfected to infected and removed extreme outliers (absolute value $\log_2$ fold change >25) or simulations that resulted in population cycles. We then performed a permutation test with 10,000 permutations (due to nonnormality of data) on the difference in mean $\log_2$ fold change of equilibrium density between planktotrophic and lecithotrophic echinoderms. We only tested for developmental mode within Echinodermata because of much lower sample sizes in Annelida and Mollusca.

Infection by a microbial manipulator often comes at a fitness cost (Engelstädter and Hurst 2009*a*). To determine how this cost caused by a feminizing microbe influences infectability, we repeated simulations for a subset of egg
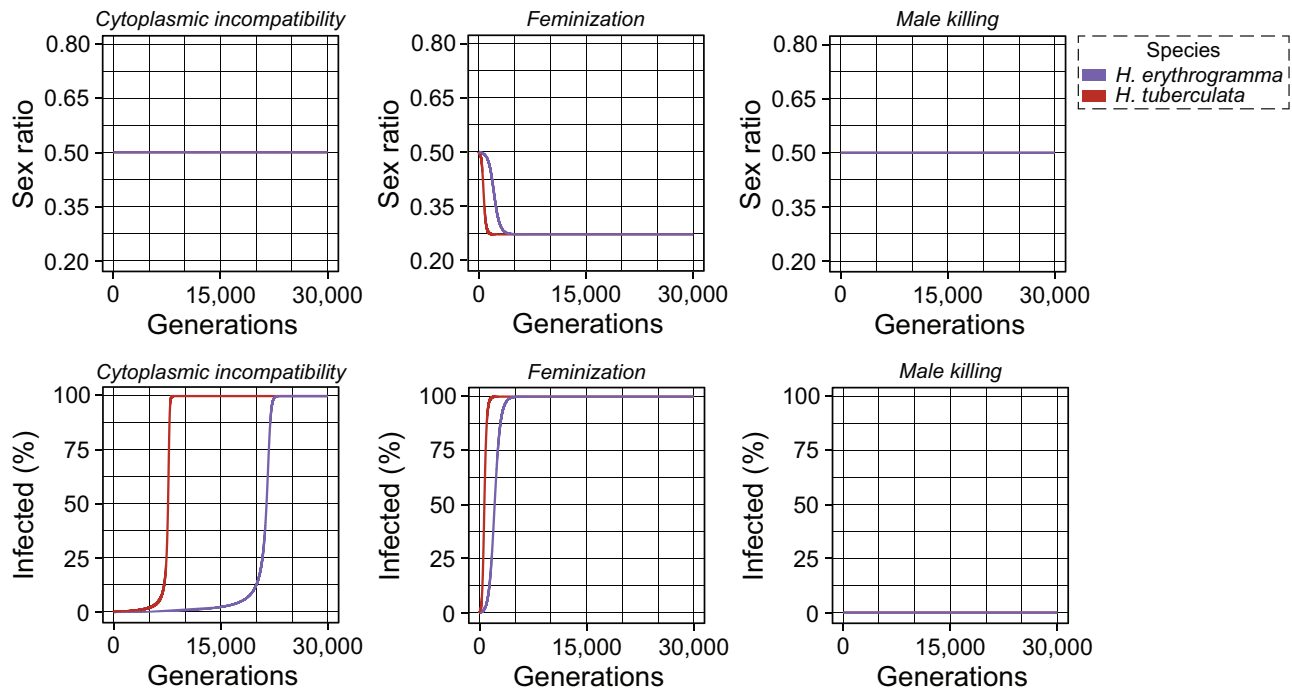
Figure 2: Sex ratio and infection dynamics during the spread of a microbial reproductive manipulator for two species of free-spawning marine invertebrates with alternative life history strategies. Shown are numerical simulations of host sex ratio (with male and female bias being >0.5 and <0.5, respectively; *top*) and proportion infected over time (*bottom*) for the planktotrophic *Heliocidaris tuberculata* (red) and lecithotrophic *H. erythrogramma* (purple) when a microbe that induces cytoplasmic incompatibility (*left*), feminization (*center*), and male killing (*right*) spreads within the population. These simulations use a population model without stage structure (see eqq. [6]–[11]) and start with a naive population (1% infected). Parameter values used are provided in tables 1 and 2, and additional simulations can be generated using the web application at https://mck8dg.shinyapps.io/SI_sex_ratio_distortion_marine_inverts/.

sizes and pelagic larval durations while varying the feminization rate and cost. Specifically, we simulated different feminization rates (r) from 0.501 to 1.000 at increments of 0.001 and costs (c) ranging from 0.000 to 0.600 at increments of 0.001. The subset of egg sizes that we used was from 450 to 800 μm at increments of 50 μm, and the subset of pelagic larval durations was 1, 5, 9, 13, 18, and 30 days. These combinations of egg size and pelagic larval duration were usually "infectable" in a preliminary feminization rate-cost analysis using a broader range of egg sizes and pelagic larval durations from above (fig. S3). Last, we tested which feminization rate and cost combinations resulted in populations with ≥99.9% infection.

## Results

Fertilization Dynamics in Free-Spawning Marine Invertebrates

Consistent with previous reports, the fertilization success and zygote production of free-spawning marine invertebrates is dependent on adult density (Pennington 1985; Levitan 1991) and egg size (Farley and Levitan 2001; Po-

dolsky 2002). Fertilization success and zygote production are also influenced by sex ratio for both the planktotrophic *Heliocidaris tuberculata* and the lecithotrophic *H. erythrogramma*, but how they are influenced depends on the developmental strategy (figs. 1, S4, S5).

In *H. tuberculata*, fertilization success is sperm limited at low adult densities (<0.01 individuals/m²) for all sex ratios until a sufficient density caused the fertilization success to reach a relative maximum. The adult density at which fertilization success reached a relative maximum depended on the sex ratio, such that the density is slightly lower in female-dominant populations (0.0177 individuals/m², for a sex ratio of 0.1) and slightly higher in male-dominant populations (0.0181 individuals/m², for a sex ratio of 0.9; figs. 1, S4, S5). The magnitude of this relative maximum in fertilization also depended on the sex ratio, whereby fertilization increased approximately linearly from 0% in a fully female population to 95% in a population that is 75% males and gradually plateaued toward a 100% fertilization success as the population became predominately, but not entirely, male (fig. S5). Within the range of realistic densities (i.e., <100 individuals/m²), polyspermy did not result in zero fertilization success until densities were
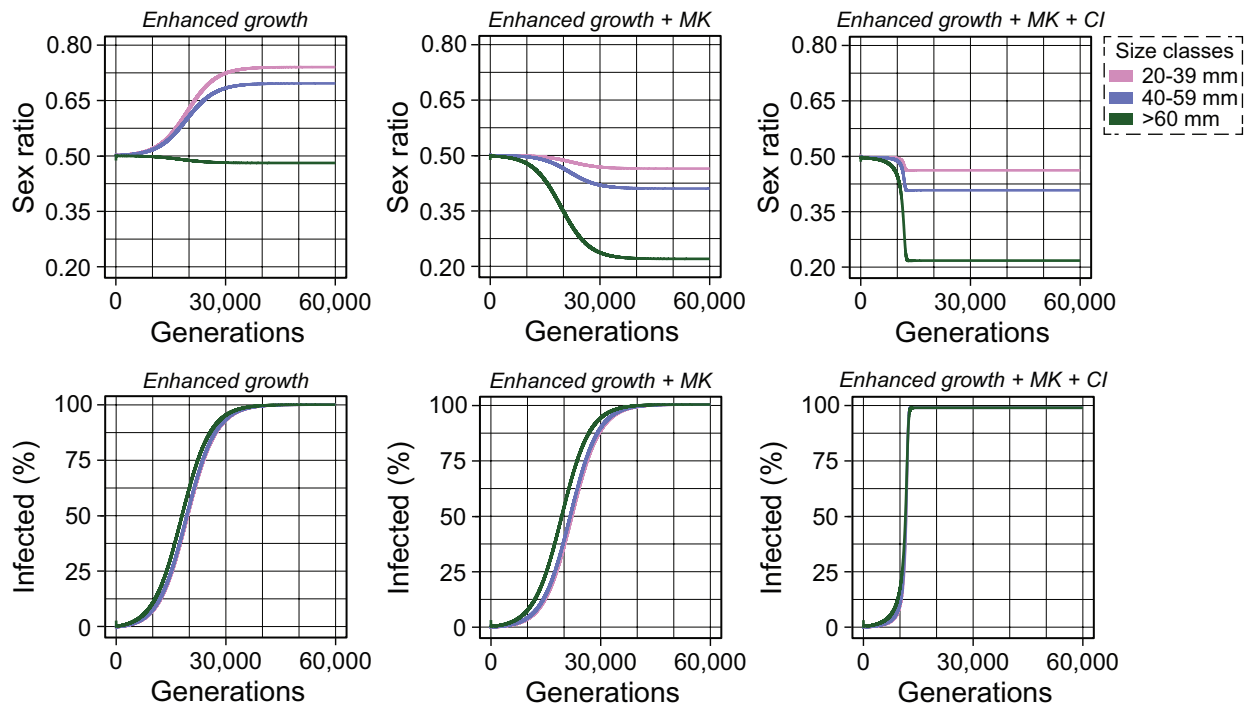
Figure 3: Sex ratio and population structure during the spread of a microbial reproductive manipulator for *Heliocidaris erythrogramma*. Shown are numerical simulations of host sex ratio (with male and female bias being >0.5 and <0.5, respectively; *top*) and proportion infected over time (*bottom*) when a microbe that enhances growth (*left*), enhances growth and incudes male killing (*center*), and enhances growth, incudes male killing, and causes cytoplasmic incompatibility (*right*) spreads within a population. These simulations use a stage-based population model and start with a naive population (1% infected) where all individuals are in the smallest size class (see eqq. [6], [7], and [12]–[20]). Parameter values used are provided in tables 1–3, and additional simulations can be generated using the web application at https://mck8dg.shinyapps.io/SI_sex_ratio_distortion_marine_inverts/. CI = cytoplasmic incompatibility; MK = male killing.

sufficiently high (>20 individuals/m²) and the sex ratio was heavily male biased (i.e., ≥0.84; figs. 1, S4, S5). For most sex ratios, however, fertilization success declined slightly as density increased (fig. 1). The interaction between density and sex ratio resulted in a greater zygote production as density increased for sex ratios below ∼0.84, even if maximum fertilization was not achieved (figs. 1, S4, S5). As the population transitioned toward female dominance, the maximum zygote production increased until 0.41, after which maximum zygote production decreased as a result of sperm limitation (figs. 1, S4, S5).

The dynamics of fertilization success and zygote production for the lecithotrophic *H. erythrogramma* were quite different. While the density-dependent fertilization success was similar in heavily male-biased populations for both *Heliocidaris* species (i.e., at 0.9), this model predicted a shift toward high adult densities—instead of a reduction—in the fertilization profile as the population structure became female biased (figs. 1, S4, S5). Maximum fertilization success stayed at 100% until the population consisted solely of females (figs. 1, S5). In the near absence of a reduc-

tion in fertilization success due to a shift in sex ratio, *H. erythrogramma* experienced an exponential increase in zygote production as the population became female dominant (figs. 1, S4, S5). Moreover, peak zygote production also shifted with the population structure and with adult density, resulting in a synergistic effect on zygote production for this developmental strategy (figs. 1, S4).

Spread of Reproductive Manipulators: A Heliocidaris *Case Study*

Our integrated model predicted that both cytoplasmic incompatibility and feminization are viable mechanisms to spread microbes that manipulate reproduction for both the planktotrophic *H. tuberculata* and the lecithotrophic *H. erythrogramma*, but male killing is not (figs. 2, S6). For both types of reproductive manipulation, infection spread and reached fixation more quickly in *H. tuberculata* than in *H. erythrogramma*. This is likely due to the fecundity difference and relatively higher zygote production in the planktotrophic *H. tuberculata* (figs. 1, S6; table 1). However,
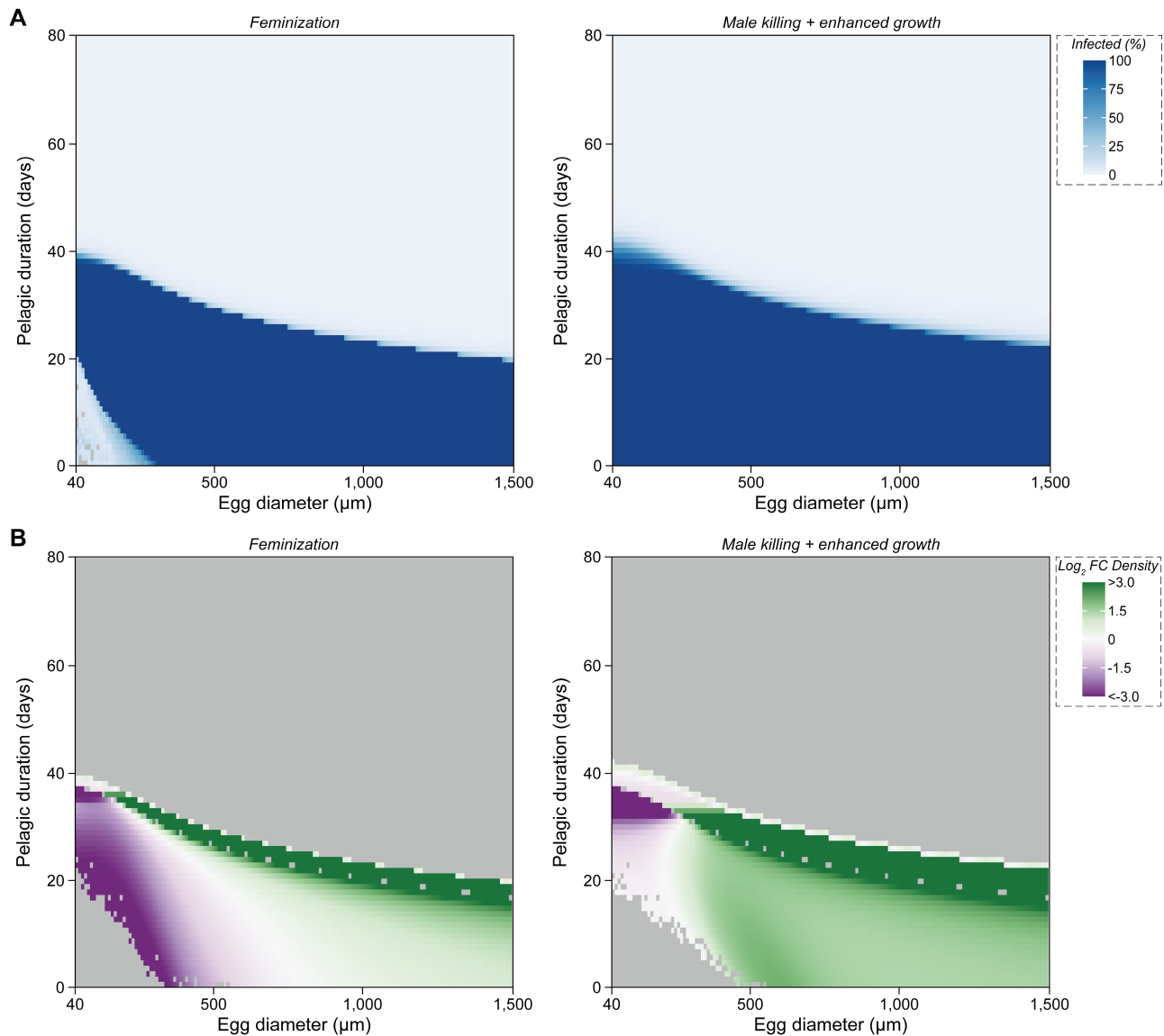
Figure 4: Equilibrium infection rate (*A*) and log$_2$ fold change in density (*B*) by a microbe that induces feminization (*left*) or male killing plus enhanced growth (*right*) at different combinations of egg diameter (from 40 to 1,500 μm with 10-μm increments) and pelagic larval duration (from 0 to 80 days with 1-day increments). Numerical simulations to determine the equilibrium were performed using equations (6)–(11). For infection rate (*A*), light through dark blue represent 0% to 100% infected, and gray boxes indicate parameter combinations that resulted in numerical errors because of too high of a growth rate. For the log$_2$ fold change in equilibrium density (individuals/m²; *B*), green through purple represent a net benefit to net cost to an infection. Moreover, gray boxes indicate parameter combinations that had less than 25% infection, had population cycles, or resulted in numerical errors because of too high of a growth rate. For this model, egg density was inversely proportional to egg diameter (Smith and Fretwell 1974). For the feminization numerical simulation (*left*), the cost of infection was 0 and the feminization rate was 0.7. For the male killing plus enhanced growth numerical simulations (*right*), the cost of infection was −1.25—representing a benefit—and the male killing rate was 0.7. Other parameters of the model were held to be the same as *Heliocidaris erythrogramma* (see table 1). Numerical simulations repeating this analysis but varying feminization and cost are shown in figure S3. The time it took to reach equilibrium, total population density at equilibrium, and the location of marine invertebrate species based on these two life history parameters can be explored in the web application at https://mck8dg.shinyapps.io/SI_sex_ratio_distortion_marine_inverts/. FC = fold change.

feminization was the only mechanism that resulted in both the infection spreading and a female-biased sex ratio.

Male killing often evolves when the female offspring is provided a benefit from the sacrificed male offspring (e.g.,

by cannibalization; Hurst et al. 1996; Engelstädter and Hurst 2009*b*). This was not present in our integrated model because the dilute lifestyle of sibling larvae for free-spawning marine invertebrates makes cannibalism highly unlikely.
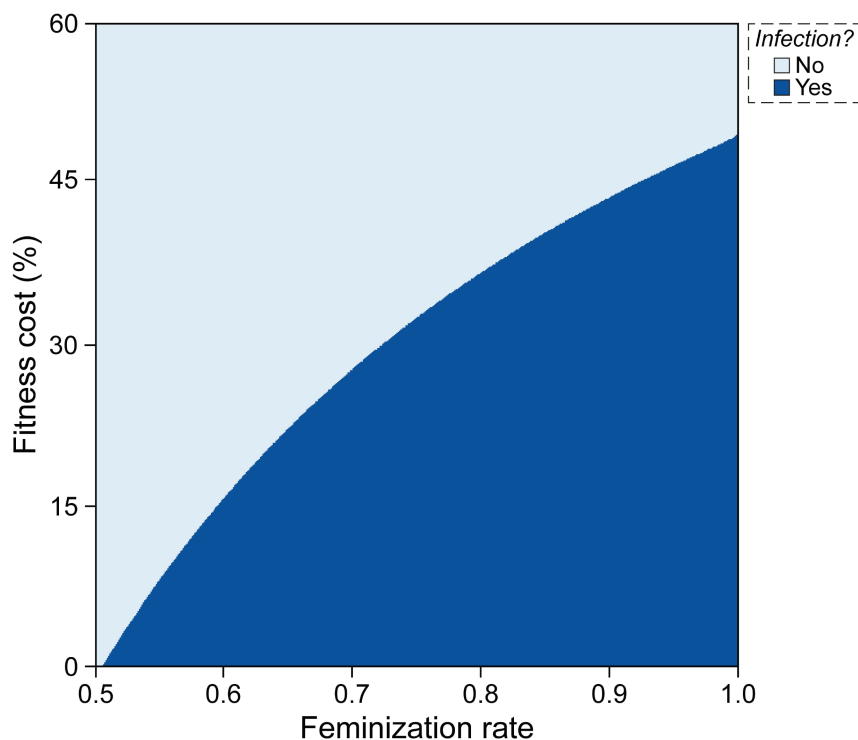
Figure 5: The combination of fitness cost and feminization rate that are predicted to result in populations with a ≥99.9% infection rate. These numerical simulations were run at feminization rates from 0.501 to 1.000 (with increments of 0.001) and costs from 0.000 to 0.600 (with increments of 0.001) for egg sizes from 450 to 800 μm (with increments of 50 μm) and pelagic larval durations of 1, 5, 9, 13, 18, and 30 days. Additional parameters of this simulation were held to those of *Heliocidaris erythrogramma* (see table 1; fig. 4).

Therefore, we provided infected females with a fitness compensation by expediting growth as an alternative mechanism for endosymbiont spread (Carrier et al. 2021). Our structured population model for both *Heliocidaris* species found that reproductive manipulators spread when enhanced growth is relatively small and higher growth rates alone resulted in male-dominant populations, with the smaller size classes being more male biased than the largest size class (figs. 3, S7–S9). When combined with a modest degree of male killing (i.e., 0.7), the population structure for each size class became female dominant, with the magnitude of this sex ratio distortion increasing with adult size (figs. 3, S7–S9). Furthermore, enhanced growth and male killing interact to affect equilibrium sex ratios, where enhanced growth influenced smaller size classes and lead to a male-biased population while male killing became more influential in the larger size classes to sway the population toward females (S8, S9). This resulted in a nearly identical population structure to that of *H. erythrogramma* in Sydney Harbor but was considerably more female dominant than is observed for *H. tuberculata* (Carrier et al. 2021). These processes were expedited to equilibrium when combined with cytoplasmic incompatibility (figs. 3, S7, S9).

Numerical Analyses of Reproductive Manipulators and Life History Traits

Our simulations across a range of egg sizes and pelagic larval durations found that combinations of egg size and larval duration served as indicators of a potential infection, whereby species of free-spawning marine invertebrates were either fully infected or not infected, with little in between (fig. 4). Of these two life history traits, the spread of a manipulating microbe was more limited by the pelagic larval duration than by egg size. Specifically, infection did not occur for larvae that spent more than ~40 days in the water column but continued beyond egg diameters of 1,500 μm (fig. 4A). The upper-bound limit of infectability was similar for a microbe that feminized the host as well as provided a fecundity benefit (i.e., enhanced growth) to the host plus male killing (fig. 4A). Furthermore, combinations with an egg size smaller than 30 μm and a pelagic duration less than 20 days also were not infectable by microbes that feminize the host. This lower limit was not present for a microbe that elicits male killing plus enhances growth, and thus this microbial strategy could infect a wider range of life history combinations than a feminizing microbe.

For the numerical analysis of a feminizing microbe, we found that 68.1% of these species fell within this "infection zone" (fig. 4A; web application at https://mck8dg.shiny apps.io/SI_sex_ratio_distortion_marine_inverts/). Phylum, but not developmental mode, was a significant predictor of infectability (phylum: $\chi_2^2 = 8.184, P = .017$; developmental mode: $\chi_1^2 = 1.754, P = .185$). Specifically, 36.8% of annelids ($n = 19$), 70.0% of echinoderms ($n = 140$), and 72.6% of molluscs ($n = 73$) as well as 71.4% of planktotrophs ($n = 154$) and 61.5% of lecithotrophs ($n = 78$) were within this zone. Furthermore, there was a significant interaction between phylum and developmental mode ($\chi_2^2 = 27.6167, P < .001$), such that lecithotrophic annelids, planktotrophic echinoderms, and lecithotrophic molluscs were less likely to fall within this infection zone than the alternative developmental strategy for each phylum (fig. S10A). Infection tended to have a negative influence on the population density of planktotrophs and a positive influence on that of lecithotrophs (fig. 4B). Moreover, within echinoderms, infection had a more positive influence on population density for lecithotrophs than for planktotrophs (mean difference in $\log_2$ fold change $= 1.223; P = .002$; fig. S11A).

For the numerical analysis of a microbe that elicits male killing plus enhances growth, we found that 83.6% of these species fell within this infection zone (fig. 4A). Phylum was the only statistically significant predictor of infectability (phylum: $\chi_2^2 = 14.605, P < .001$; developmental mode: $\chi_1^2 = 2.997, P = .083$; interaction: $\chi_2^2 = 0.562, P = .756$). Specifically, 100% of annelids ($n = 19$), 77.9% of echinoderms ($n = 140$), and 90.4% of molluscs ($n = 73$) as well as 81.8% of planktotrophs ($n = 154$) and 87.2% of lecithotrophs ($n = 78$) were within this zone (fig. S10B). Infections tended to have a negative influence on the population density of planktotrophs and a positive influence on that of lecithotrophs (fig. 4B), and this was particularly the case for echinoderms (mean difference in $\log_2$ fold change $= 2.308, P < .001$; fig. S11B).

The shape of this infection zone was constant across all combinations of feminization rate and infection cost (fig. S3). After a certain cost, however, the potential for an infection across all life history combinations fell to zero, and thus this infection zone disappeared completely (fig. S3). There was a clear boundary for the maximum cost that a reproductive manipulator can incur on its host given a fixed feminization rate, resulting in a hyperbolic relationship between these factors (fig. 5). In other words, there is a fine balance between the feminization rate, fitness cost to the host, and whether an infection may occur.

Discussion

We integrated two types of models—the first on the fertilization dynamics of free spawning and the second on the consequences of cytoplasmic incompatibility, feminization, and male killing—to understand whether microbes that manipulate host reproduction spread within populations of free-spawning marine invertebrates and distort their sex ratio. Our model and the *Heliocidaris* case study support three primary findings. First, sex ratio distortion leads to suboptimal fertilization and zygote production in planktotrophs but can enhance these processes in lecithotrophs. Second, feminization and a combination of male killing plus enhanced growth are effective at spreading reproductive manipulators while also inducing a female-biased sex ratio. Third, the majority of free-spawning marine invertebrates could be infected across a range of fitness costs and manipulation rates, with infections favoring and benefitting species with larger eggs and shorter pelagic durations. These results suggest that the life history evolution of free-spawning marine invertebrates is an underlying factor in whether microbes that manipulate reproduction may infect and spread these partnerships.

Life History Evolution and Microbes That Manipulate Reproduction

The reproductive success of free-spawning marine invertebrates is often limited by sperm availability, which may be partially offset by increasing egg size, increasing spawning density, and spawning in synchrony (Pennington 1985; Levitan et al. 1992; Oliver and Babcock 1992; Levitan and Petersen 1995; Yund 2000; Levitan 2006). An additional mechanism that may limit reproductive success is the distortion of host sex ratio toward female dominance. This population structure is common for some groups of free-spawning marine invertebrates (Carrier et al. 2021), implying that it may provide some benefits. Our fertilization model is in agreement with this statement. The planktotroph in our case study experienced a lower maximum fertilization success as the sex ratio became more female biased, while maximum zygote production increased as the sex ratio became slightly female biased but decreased thereafter. Fertilization curves of the lecithotroph, on the other hand, were constant across sex ratios and shifted slightly toward higher adult densities. This, in turn, resulted in a maximum fertilization success of ~100% for most sex ratios and an exponential increase in the maximum zygote production as sex ratio became more female biased.

An increase in zygote production would benefit the host as well as the reproductive manipulator (Engelstädter and Hurst 2009a), but this fitness advantage is inconsistent across the life history strategy of the host. If a reproductive manipulator that distorts host sex ratio were to infect a planktotrophic species, then the high fecundity of this life history strategy alone should promote the rapid spread

of the microbe. Transitioning from a male-dominant to a female-dominant population structure would provide an initial fitness benefit, but if the selective pressures on host reproduction are too high, then the manipulator would succumb to its own influence. For the planktotrophic life history strategy, host sex ratio appears to parallel the mutualism-parasite continuum, such that a mild reproductive manipulator could be beneficial while a highly effective one would be parasitic, with limitations to reproductive success being at fertilization. This continuum is widely observed in terrestrial arthropods (Hatcher et al. 1999; Charlat et al. 2007; Drew et al. 2021) and appears possible in the sea.

Infecting planktotrophs should also be an ineffective transmission route for microbial manipulators. Natural mortality of marine invertebrate larvae is generally dependent on the time spent in the water column. Gamete wastage (mortality) often exceeds 90%–95% because planktotrophic larvae spend weeks in the water column, and thus this would compromise the fitness of a reproductive manipulator at a rate equal to host mortality (Thorson 1950; Young and Chia 1987; Rumrill 1990; Morgan 1995; Engelstädter and Hurst 2009*a*). For example, if a planktotrophic larval host spends a mere 21 days in the water column, then only ~0.1% of the reproductive manipulator cells would be transmitted to the next generation (Strathmann 1985; Rumrill 1990). This limitation is based on the pelagic duration of the larva and is reflected in our numerical analyses that predicts the infectable life history combinations (Shanks 2009). Specifically, while ~68% (feminization) to ~84% (enhanced growth plus male killing) of species could be infectable, those with shorter pelagic larval durations and larger maternal investment (egg size) were favored and should benefit from an infection. Maternal investment also happens to be a strong proxy for the developmental life history strategy of free-spawning marine invertebrates (Thorson 1950; Vance 1973; Emlet et al. 1987).

Lecithotrophic species produce fewer, but substantially larger, eggs than planktotrophs, and the resulting larvae spend only days in the water column (Thorson 1950; Emlet et al. 1987; Shanks 2009). If a reproductive manipulator that distorts host sex ratio were to infect a lecithotroph, then the symbiont could benefit from the eggs physical size by substantially increasing its initial titer and minimize a fitness loss because this developmental strategy spends a brief period in the water column. Distorting the sex ratio of this life history strategy could favor an exponential increase in zygote production that would be advantageous for both the host and the reproductive manipulator. Opposing that of planktotrophs, associations between lecithotrophs and reproductive manipulators could be perceived as a mutualism that would likely be more stable and increasingly beneficial as the host sex ratio is distorted toward a female-dominant population structure.

Provided the differences in infection limitations and benefits to these two life history strategies for a reproductive manipulator, it may be hypothesized that these microbes could serve as selective agents to induce, mediate, and/or reinforce transitions between the developmental strategies of free-spawning marine invertebrates. Life history transitions between these developmental strategies have occurred in several major animal lineages, with rapid evolutionary shifts from planktotrophy to lecithotrophy being well documented. It is thought that an increase in the energetic content (size) of the egg relaxes the selective pressure maintaining the feeding structures and that development to metamorphosis is accelerated once these are lost (Strathmann 1978, 1985; Wray and Raff 1991*a*; Raff 1992; Jaeckle 1995; Wray 1996; McEdward and Morgan 2001; Sewell and Manahan 2001; Raff and Byrne 2006; Moran et al. 2013). An increase in egg size and an accelerated time to metamorphosis would both favor the likelihood that a reproductive manipulator is transmitted to the subsequent generation. If such microbes also distort the host's sex ratio, then there would be multiple incentives to induce, mediate, and/or reinforce transitions in the developmental life history of free-spawning marine invertebrates.

Spread and Influence of Marine Reproductive Manipulators

Microbes that manipulate reproduction in terrestrial systems spread by cytoplasmic incompatibility, feminization, and male killing, but only feminization and male killing may distort host sex ratio (Engelstädter and Hurst 2009*a*). Our model suggests that the reproduction of free-spawning marine invertebrates may be influenced by each of these; that host sex ratio may be distorted by feminization and male killing, with the latter occurring only when the host receives some enhanced growth benefit (i.e., fecundity benefit); and that cytoplasmic incompatibility enhances the spread of these microbes. In all cases, reproductive manipulators also spread faster in planktotrophs than in lecithotrophs. Therefore, we suspect some convergence between microbe-mediated reproductive manipulation on land and in the sea. The prevailing question is, how may these occur in marine systems?

Feminization involves the conversion of males to females by microbes that interact with the host's sex determination system. This is similar to sequential hermaphroditism, except that feminization is mediated by the microbial manipulator. It is common for free-spawning marine invertebrates to be sequential hermaphrodites (Sewell 1994; Collin 2006). The patterns and timing of sex change in echinoderms, for example, varies considerably and may occur in either direction, with protandry being more prevalent (see table 1

in Sewell 1994). One expectation of marine microbial manipulators is that they would interfere with the sex determination system of a sequential hermaphrodite to enable an earlier transition from male to female (Warner 1975; Munday et al. 2006). This type of reproductive manipulation has the potential to be widespread in marine invertebrates and likely depends on the capacity of these microbes to interfere with the sex determination systems for free-spawning marine invertebrates.

Male killing, on the other hand, involves microbes that cause an elevated mortality during male development and can primarily help the spread of infection when females can benefit directly from the sacrificed siblings (Hurst and Jiggins 2000). This type of reproductive manipulation alone appears unlikely for free-spawning marine invertebrates for two reasons. First, embryonic mortality naturally exceeds 90%–95% and mortality due to male killing would be an additional 5%–90% (Young and Chia 1987; Rumrill 1990; Morgan 1995; Pechenik 1999; Hurst and Jiggins 2000; Engelstädter and Hurst 2009a). The combination of these mortality sources would be overwhelming and, unlike terrestrial systems, would limit microbial fitness in addition to the host. Second, life in the plankton for the offspring of free-spawning marine invertebrates is an independent endeavor, and this would not allow for a fitness compensation. We suspect that male killing may evolve in the benthic (adult) life stage, which would be a type of male killing that is not observed in terrestrial systems (Engelstädter and Hurst 2009a). Alternatively, a potential ecological "hot spot" where male killing may evolve is when offspring are brooded, thereby being confined and where sibling cannibalism is observed (e.g., echinoderms [Byrne 1996] and gastropods [Strathmann and Strathmann 2006).

An alternative mechanism to compensate for the fitness cost related to male killing is by the microbe supplementing host nutrition. Under this circumstance in our model, male killing appeared to be stable for the lecithotroph and able to elicit a shift in sex ratio toward female dominance, and such a microbe was able to infect a larger range of life history combinations than a feminizing microbe. Moreover, when modeled with enhanced growth in a size-structured population, this combination resulted in a population structure highly similar to that observed in the field for the lecithotroph (Carrier et al. 2021). If only provided a growth benefit, then the population became male dominant, which was accelerated with cytoplasmic incompatibility. Therefore, male killing coupled with some growth (i.e., nutritional) benefit that should increase host fitness and promote the spread of the symbiont. The free-floating life of the developmental stages of marine invertebrates may thus be influenced by such reproductive manipulators.

An additional mechanism of microbial manipulation is cytoplasmic incompatibility (Engelstädter and Telschow 2009). This common type of reproductive manipulation enhances symbiont spread by eliciting embryonic mortality when infected males mate with uninfected females but avoids this when both sexes carry the compatible manipulator. Furthermore, cytoplasmic incompatibility can be either unidirectional or bidirectional, with lethality being avoided in the latter when both sexes harbor the same strain of the symbiont. This results in reproductive isolation between hosts with different infection strains and can sufficiently restrict gene flow and induce speciation events (Engelstädter and Hurst 2009a; Shropshire et al. 2020; Kaur et al. 2021). Our model suggests that such a mechanism would enable the spread of reproductive manipulators in the sea.

Although not currently interpreted as symbiont-induced cytoplasmic incompatibly, there are a diverse array of gamete incompatibilities observed in the sea. For example, there are strong male-by-female interactions and maternal effects on fertilization efficiency and zygote success in ascidians (David et al. 2016), echinoderms (Evans and Marshall 2005), and mollusks (Rawson et al. 2003). The hypothesized causal mechanisms for these examples stem from a host point of view, but these processes may also be caused by a microbial manipulator. Our model demonstrates that cytoplasmic incompatibility is a viable mechanism for a symbiont to spread in the sea, and we propose this alternative view should also be considered. We believe this is especially true when a unidirectional or bidirectional incompatibility is suspected (Shropshire et al. 2020). In the case of incompatibilities, the microbial community should then be profiled, and if a Rickettsiales is a dominant member of the gonad and egg-associated microbiome, then a reproductive manipulator may be present.

Was the Life History Evolution of Heliocidaris a Reproductive Manipulation?

If the life history evolution of *Heliocidaris* has been manipulated, then our model and numerical simulations would suggest that *H. erythrogramma* (i) has a microbe that could feminize or elicit male killing if a growth benefit is provided, (ii) has an enhanced reproductive output, and (iii) has had subsequent speciation events that led to species with larger eggs and/or shorter pelagic durations. We believe that each of these expectations have been met. First, the *Echinorickettsia raffii* genome has an ankyrin protein with a homologous domain to a male killing gene and a complete shikimate pathway to biosynthesize essential amino acids that may supplement host nutrition (Carrier et al. 2021). Second, adult density in female-dominant populations in Western Australia is near the modeled maximum for zygote production and this far exceeds that of the balanced (1:1) Eastern Australia population (Dix 1977; Evans and Marshall 2005; Binks et al. 2012; Carrier et al. 2021).

Third, two subsequent speciation events occurred as *H. erythrogramma* spread. One of these species (*H. bajulus*) has large eggs that are brooded and undergo a lecithotrophic development in a thick gelatinous coat adhered to the parent (Dartnall 1972; McMillan et al. 1992; Zigler et al. 2003; Hart et al. 2011, 2012). The natural history and life history evolution of *Heliocidaris* is therefore consistent with expectations of a reproductive manipulation in the sea.

Male killing would seem to be the likely type of reproductive manipulation that influenced the life history evolution of *Heliocidaris*. Our model, however, showed that cytoplasmic incompatibility could be viable in combination with this mechanism, and we suspect it occurs as well. First, there is unidirectional hybrid incompatibility, where *H. tuberculata* sperm bind to but cannot fertilize *H. erythrogramma* eggs unless the jelly coat is removed, allowing for a fertilization efficiency (~85%) equal to the reciprocal cross (Raff et al. 1999; Zigler et al. 2003). Second, while both sexes contribute to the high degree of fertilization success within populations, there is a substantial maternal effect in this system (Evans and Marshall 2005; Evans et al. 2007). Third, since spreading to Western Australia, *H. erythrogramma* has subspeciated to *H. e. erythrogramma* and *H. e. armigera*, and these can, but rarely do, hybridize because of asynchrony in the spawning seasons (McMillan et al. 1992; Binks 2011; Binks et al. 2012). Therefore, we hypothesize that the reproductive and population biology of *H. erythrogramma* is also influenced by cytoplasmic incompatibility and that marine reproductive manipulators should have cytoplasmic incompatibility factor genes (LePage et al. 2017; Kaur et al. 2021), but these have yet to be identified.

Model Limitations and a Way Forward

Modeling the fertilization and life history dynamics of free-spawning marine invertebrates as well as reproductive manipulation are simplified here, and this may have influenced our results. There are three assumptions that we feel will need to be relaxed in future modeling efforts to more broadly understand how microbes that manipulate reproduction influence free-spawning marine invertebrates. First, our model was deterministic and, by definition, lacked stochasticity. Without this, the proportion of infected individuals can remain extremely small and eventually rise to fixation. Second, our model assumes a closed population, where an infection will still spread even if a population is not optimally productive if there is an advantage to the infected females. In an open system, a more productive neighboring population that was uninfected could swamp the population with a nascent infection and prevent the infection from spreading. Such a dynamic would likely be more important for planktotrophs than lecithotrophs because sex ratio distortion easily moves these species off their optimum and migration rates and gene flow are likely high (McMillan et al. 1992). Third, our model does not address the possibility for variation among individuals and, thus, for the evolution of reproductive traits that influence symbiont spread. It is likely that changes in sex ratio or, more specifically, the egg-to-sperm ratio influence the selection on reproductive traits (e.g., egg size and sperm velocity). Changes in host reproductive traits may enhance or prevent the spread of a reproductive manipulator. Explicitly modeling the potential coevolution between host and symbiont is needed to test the hypothesis that symbionts may mediate transitions in the developmental life history of free-spawning marine invertebrates.

Conclusions

Our model supports the general premise that microbes may manipulate the reproduction of free-spawning marine invertebrates and that the types of manipulation overlap considerably with terrestrial systems (Hatcher et al. 1999; Charlat et al. 2007). Much of the life history landscape of free-spawning marine invertebrates may be manipulated by these microbes. The reality of a manipulation likely differs considerably for a host with different life history strategies, such that stable and beneficial shifts in population structure may be induced for lecithotrophs while there are limitations to reproductive success for planktotrophs. This begs the question of whether reproductive manipulators are omnipresent in the sea as they are on land, whether there are geographical and life history hot spots for these microbes, and whether the aquatic environment features unique ways for microbes to manipulate host reproduction.

Statement of Authorship

M.C.K and T.J.C. conceptualized the study. T.J.C. collected data for model parameter fitting. M.C.K. developed the equations for the model, coded the model, and ran all analyses.

M.C.K. made initial figures, and T.J.C. touched up figures. Both authors discussed the results and wrote the manuscript.

Data and Code Availability

Code and data needed to run the model, make figures, and perform statistical analyses have been deposited in the Dryad Digital Repository (https://doi.org/10.7291/D15Q4X; Kustra and Carrier 2022).

Literature Cited

Allen, J., and B. Pernet. 2007. Intermediate modes of larval development: bridging the gap between planktotrophy and lecithotrophy. Evolution and Development 9:643–653.

Álvarez-Noriega, M., S. Burgess, J. Byers, J. Pringle, J. Wares, and D. Marshall. 2020. Global biogeography of marine dispersal potential. Nature Ecology and Evolution 4:1196–1203.

Ammar, E.-D., and S. Hogenhout. 2006. Mollicutes associated with arthropods and plants. Pages 119–140 *in* K. Bourtzis and T. Miller, eds. Insect symbiosis. CRC, Boca Raton, FL.

Bates, J., E. Mittge, J. Kuhlman, K. Baden, S. Cheesman, and K. Guillemin. 2006. Distinct signals from the microbiota promote different aspects of zebrafish gut differentiation. Developmental Biology 297:374–386.

Binet, M., and C. Doyle. 2013. Effect of near-future seawater temperature rises on sea urchin sperm longevity. Marine and Freshwater Research 64:1–9.

Binks, R. 2011. Investigating the evolutionary significance of morphological variation in the Australian sea urchin *Heliocidaris erythrogramma*. PhD thesis. University of Western Australia.

Binks, R., J. Prince, J. Evans, and W. Kennington. 2012. More than bindin divergence: reproductive isolation between sympatric subspecies of a sea urchin by asynchronous spawning. Evolution 66:3545–3557.

Bosch, T., and M. McFall-Ngai. 2021. Animal development in the microbial world: re-thinking the conceptual framework. Current Topics in Developmental Biology 141:399–427.

Bright, M., and S. Bulgheresi. 2010. A complex journey: transmission of microbial symbionts. Nature Reviews Microbiology 8:218–230.

Burgess, S., M. Baskett, R. Grosberg, S. Morgan, and R. Strathmann. 2015. When is dispersal for dispersal? unifying marine and terrestrial perspectives. Biological Reviews 91:867–882.

Byrne, M. 1996. Viviparity and intragonadal cannibalism in the diminutive sea stars *Patiriella vivipara* and *P. parvivipara* (family Asterinidae). Marine Biology 125:551–567.

———. 2006. Life history diversity and evolution in the Asterinidae. Integrative and Comparative Biology 46:243–254.

Byrne, M., J. Villinski, P. Cisternas, R. Siegel, E. Popodi, and R. Raff. 1999. Maternal factors and the evolution of developmental mode: evolution of oogenesis in *Heliocidaris erythrogramma*. Development Genes and Evolution 209:275–283.

Callaini, G., M. Riparbelli, and R. Dallai. 1994. The distribution of cytoplasmic bacteria in the early *Drosophila* embryo is mediated by astral microtubules. Journal of Cell Science 107:673–682.

Carrier, T., B. Leigh, D. Deaker, H. Devens, G. Wray, S. Bordenstein, M. Byrne, et al. 2021. Microbiome reduction and endosymbiont gain from a switch in sea urchin life history. Proceedings of the National Academy of Sciences of the USA 118:e2022023118.

Charlat, S., E. Hornett, J. Fullard, J. Davies, G. Roderick, N. Wedell, and G. Hurst. 2007. Extraordinary flux in sex ratio. Science 317:214.

Collin, R. 2006. Sex ratio, life-history invariants, and patterns of sex change in a family of protandrous gastropods. Evolution 60:735–745.

Dartnall, A. 1972. A brooding echinoid from Tasmania. Proceedings of the Linnean Society of New South Wales 96:30–34.

David, A., M. Blows, and D. Marshall. 2016. Genetic compatibility underlies benefits of mate choice in an external fertilizer. American Naturalist 187:647–657.

Dix, T. 1977. Reproduction in Tasmanian populations of *Heliocidaris erythrogramma* (Echinodermata: Echinometridae). Australian Journal of Marine and Freshwater Research 28:509–520.

Douglas, A. 1998. Nutritional interactions in insect-microbial symbioses: aphids and their symbiotic bacteria *Buchnera*. Annual Review of Entomology 43:17–37.

Drew, G., E. Stevens, and K. King. 2021. Microbial evolution and transitions along the parasite–mutualist continuum. Nature Reviews Microbiology 19:623–638.

Duron, O., D. Bouchon, S. Boutin, L. Bellamy, L. Zhou, J. Engelstädter, and G. Hurst. 2008. The diversity of reproductive parasites among arthropods: *Wolbachia* do not walk alone. BMC Biology 6:27.

Emlet, R., and O. Hoegh-Guldberg. 1997. Effects of egg size on postlarval performance: experimental evidence from a sea urchin. Evolution 51:141–152.

Emlet, R., L. McEdward, and R. Strathmann. 1987. Echinoderm larval ecology viewed from the egg. Pages 55–136 *in* M. Jangoux and J. M. Lawrence, eds. Echinoderm studies. Vol. 2. CRC, Boca Raton, FL.

Engelmann, F. 2015. The physiology of insect reproduction. International Series of Monographs in Pure and Applied Biology. Elsevier, Amsterdam.

Engelstädter, J., and G. Hurst. 2009a. The ecology and evolution of microbes that manipulate host reproduction. Annual Review of Ecology, Evolution, and Systematics 40:127–149.

———. 2009b. What use are male hosts? the dynamics of maternally inherited bacteria showing sexual transmission or male killing. American Naturalist 173:E159–E170.

Engelstädter, J., and A. Telschow. 2009. Cytoplasmic incompatibility and host population structure. Heredity 103:196–207.

Evans, J., F. Garcia-Gonzalez, and D. Marshall. 2007. Sources of genetic and phenotypic variance in fertilization rates and larval traits in a sea urchin. Evolution 61:2832–2838.

Evans, J., and R. Lymbery. 2020. Sexual selection after gamete release in broadcast spawning invertebrates. Philosophical Transactions of the Royal Society B 375:20200069.

Evans, J., and D. Marshall. 2005. Male-by-female interactions influence fertilization success and mediate the benefits of polyandry in the sea urchin *Heliocidaris erythrogramma*. Evolution 59:106–112.

Farley, G., and D. Levitan. 2001. The role of jelly coats in sperm-egg encounters, fertilization success, and selection on egg size in echinoids. American Naturalist 157:626–636.

Fitzpatrick, J., F. Garcia-Gonzalez, and J. Evans. 2010. Linking sperm length and velocity: the importance of intramale variation. Biology Letters 6:797–799.

Foo, S., D. Deaker, and M. Byrne. 2018. Cherchez la femme—impact of ocean acidification on the egg jelly coat and attractants for sperm. Journal of Experimental Biology 221:jeb177188.

Fraune, S., and T. Bosch. 2010. Why bacteria matter in animal development and evolution. BioEssays 32:571–580.

Giese, A. 1959. Comparative physiology: annual reproductive cycles of marine invertebrates. Annual Review of Physiology 21:547–576.

Gilbert, S., T. Bosch, and C. Ledon-Rettig. 2015. Eco-evo-devo: developmental symbiosis and developmental plasticity as evolutionary agents. Nature Reviews Genetics 16:611–622.

Hancock, P., S. Sinkins, and H. Godfray. 2011. Population dynamic models of the spread of *Wolbachia*. American Naturalist 177:323–333.

Hart, M., C. Abt, and R. Emlet. 2011. Molecular phylogeny of echinometrid sea urchins: more species of *Heliocidaris* with derived modes of reproduction. Invertebrate Biology 130:175–185.

Hart, M., I. Popovic, and R. Emlet. 2012. Low rates of bindin codon evolution in lecithotrophic *Heliocidaris* sea urchins. Evolution 66:1709–1721.

Harumoto, T., and B. Lemaitre. 2018. Male-killing toxin in a bacterial symbiont of *Drosophila*. Nature 557:252–255.

Hatcher, M., D. Taneyhill, and A. Dunn. 1999. Population dynamics under parasitic sex ratio distortion. Theoretical Population Biology 56:11–28.

Hilgenboecker, K., P. Hammerstein, P. Schlattmann, A. Telschow, and J. Werren. 2008. How many species are infected with *Wolbachia*? a statistical analysis of current data. FEMS Microbiology Letters 281:215–220.

Hosokawa, T., R. Koga, Y. Kikuchi, X.-Y. Meng, and T. Fukatsu. 2010. *Wolbachia* as a bacteriocyte-associated nutritional mutualist. Proceedings of the National Academy of Sciences of the USA 107:769–774.

Hurst, G., and F. Jiggins. 2000. Male-killing bacteria in insects: mechanisms, incidence, and implications. Emerging Infectious Diseases 6:329–336.

Hurst, G., L. Walker, and M. Majerus. 1996. Bacterial infections of hemocytes associated with the maternally inherited male-killing trait in British populations of the two spot ladybird, *Adalia bipunctata*. Journal of Invertebrate Pathology 68:286–292.

Israel, J., M. Martik, M. Byrne, E. Raff, R. Raff, D. McClay, and G. Wray. 2016. Comparative developmental transcriptomics reveals rewiring of a highly conserved gene regulatory network during a major life history switch in the sea urchin genus *Heliocidaris*. PLoS Biology 14:e1002391.

Jaeckle, W. B. 1995. Variation in size, energy content, and biochemical composition of invertebrate eggs: correlates to the mode of larval development. Pages 49–77 *in* L. R. McEdward, ed. Ecology of marine invertebrate larvae. CRC, Boca Raton, FL.

Jansen, V., M. Turelli, and H. Godfray. 2008. Stochastic spread of *Wolbachia*. Proceedings of the Royal Society B 275:2769–2776.

Kaur, R., J. Shropshire, K. Cross, B. Leigh, A. Mansueto, V. Stewart, S. Bordenstein, et al. 2021. Living in the endosymbiotic world of *Wolbachia*: a centennial review. Cell Host and Microbe 29:879–893.

Kitajima, E., T. Groot, and V. Novelli. 2007. *In situ* observation of the *Cardinium* symbionts of *Brevipalpus* (Acari: Tenuipalpidae) by electron microscopy. Experimental and Applied Acarology 42:263–271.

Klinges, J., S. Rosales, R. McMinds, E. Shaver, A. Shantz, E. Peters, M. Eitel, et al. 2019. Phylogenetic, genomic, and biogeographic characterization of a novel and ubiquitous marine invertebrate-associated Rickettsiales parasite, Candidatus *Aquarickettsia rohweri*, gen. nov., sp. nov. ISME Journal 13:2938–2953.

Kustra, M. C., and T. J. Carrier. 2022. Data from: On the spread of microbes that manipulate reproduction in marine invertebrates. American Naturalist, Dryad Digital Repository, https://doi.org/10.7291/D15Q4X.

Laegdsgaard, P., M. Byrne, and D. T. Anderson. 1991. Reproduction of sympatric populations of *Heliocidaris erythrogramma* and *H. tuberculata* (Echinoidea) in New South Wales. Marine Biology 110:359–374.

LePage, D., J. Metcalf, S. Bordenstein, J. On, J. Perlmutter, J. Shropshire, E. Layton, et al. 2017. Prophage WO genes recapitulate and enhance *Wolbachia*-induced cytoplasmic incompatibility. Nature 543:243–247.

Levin, L., and T. Bridges. 1995. Pattern and diversity in reproduction and development. Pages 1–48 *in* L. R. McEdward, ed. Ecology of marine invertebrate larvae. CRC, Boca Raton, FL.

Levitan, D. 1991. Influence of body size and population density on fertilization success and reproductive output in a free-spawning invertebrate. Biological Bulletin 181:261–268.

———. 1993. The importance of sperm limitation to the evolution of egg size in marine invertebrates. American Naturalist 141:517–536.

———. 1995. The ecology of fertilization in free-spawning invertebrates. Pages 123–156 *in* L. R. McEdward, ed. Ecology of marine invertebrate larvae. CRC, Boca Raton, FL.

———. 2004. Density-dependent sexual selection in external fertilizers: variances in male and female fertilization success along the continuum from sperm limitation to sexual conflict in the sea urchin *Strongylocentrotus franciscanus*. American Naturalist 164:298–309.

———. 2006. The relationship between egg size and fertilization success in broadcast-spawning marine invertebrates. Integrative and Comparative Biology 46:298–311.

Levitan, D., and C. Petersen. 1995. Sperm limitation in the sea. Trends in Ecology and Evolution 10:228–231.

Levitan, D., M. Sewell, and F.-S. Chia. 1992. How distribution and abundance influence fertilization success in the sea urchin *Strongylocentrotus franciscanus*. Ecology 73:248–254.

Ling, S., N. Kriegisch, B. Woolley, and S. Reeves. 2019. Density-dependent feedbacks, hysteresis, and demography of overgrazing sea urchins. Ecology 100:e02577.

Longo, F., J. Lynn, D. McCulloh, and E. Chambers. 1986. Correlative ultrastructural and electrophysiological studies of sperm-egg interactions of the sea urchin, *Lytechinus variegatus*. Developmental Biology 118:155–166.

Marshall, D., P. Krug, E. Kupriyanova, M. Byrne, and R. Emlet. 2012. The biogeography of marine invertebrate life histories. Annual Review of Ecology, Evolution, and Systematics 43:97–114.

May, R. 1974. Biological populations with nonoverlapping generations: stable points, stable cycles, and chaos. Science 186:645–647.

McEdward, L., and K. Morgan. 2001. Interspecific relationships between egg size and the level of parental investment per offspring in echinoderms. Biological Bulletin 200:33–50.

McFall-Ngai, M., M. Hadfield, T. Bosch, H. Carey, T. Domazet-Loso, A. Douglas, N. Dubilier, et al. 2013. Animals in a bacterial world, a new imperative for the life sciences. Proceedings of the National Academy of Sciences of the USA 110:3229–3236.

McFall-Ngai, M. J. 2002. Unseen forces: the influence of bacteria on animal development. Developmental Biology 242:1–14.

McMillan, W., R. Raff, and S. Palumbi. 1992. Population genetic consequences of developmental evolution in sea urchins (genus *Heliocidaris*). Evolution 46:1299–1312.

Mileikovsky, S. 1971. Types of larval development in marine bottom invertebrates, their distribution and ecological significance: a reevalution. Marine Biology 10:193–213.

Moran, A., J. McAlister, and E. Whitehill. 2013. Eggs as energy: revisiting the scaling of egg size and energetic content among echinoderms. Biological Bulletin 224:184–191.

Morgan, S. 1995. Life and death in the plankton: larval mortality and adaptation. Pages 279–321 *in* L. R. McEdwards, ed. Ecology of marine invertebrate larvae. CRC, Boca Raton, FL.

Morris, R., M. Rappe, S. Connon, K. Vergin, W. Siebold, C. Carlson, and S. Giovannoni. 2002. SAR11 clade dominates ocean surface bacterioplankton communities. Nature 420:806–810.

Munday, P., P. Buston, and R. Warner. 2006. Diversity and flexibility of sex-change strategies in animals. Trends in Ecology and Evolution 21:89–95.

O'Conner, C., and J. Mulley. 1977. Temperature effects on periodicity and embryology, with observations on the population genetics, of the aquacultural echinoid *Heliocidaris tuberculata*. Aquaculture 12:99–114.

Oliver, J., and R. Babcock. 1992. Aspects of the fertilization ecology of broadcast spawning corals: sperm dilution effects and *in situ* measurements of fertilization. Biological Bulletin 183:409–417.

Pechenik, J. 1999. On the advantages and disadvantages of larval stages in benthic marine invertebrate life cycles. Marine Ecology Progress Series 177:269–297.

Pennington, J. 1985. The ecology of fertilization of echinoid eggs: the consequences of sperm dilution, adult aggregation, and synchronous spawning. Biological Bulletin 169:417–430.

Perlman, S., M. Hunter, and E. Zchori-Fein. 2006. The emerging diversity of *Rickettsia*. Proceedings of the Royal Society B 273:2097–2106.

Perlmutter, J., and S. Bordenstein. 2020. Microorganisms in the reproductive tissues of arthropods. Nature Reviews Microbiology 18:97–111.

Podolsky, R. 2002. Fertilization ecology of jelly coats: physical versus chemical contributions to fertilization success of free spawned eggs. Journal of Experimental Biology 205:1657–1668.

Raff, E., E. Popodi, B. Sly, F. Turner, J. Villinski, and R. Raff. 1999. A novel ontogenetic pathway in hybrid embryos between species with different modes of development. Development 126:1937–1945.

Raff, R. 1992. Direct-developing sea urchins and the evolutionary reorganization of early development. BioEssays 12:211–218.

Raff, R., and M. Byrne. 2006. The active evolutionary lives of echinoderm larvae. Heredity 97:244–252.

Rawson, P., C. Slaughter, and P. Yund. 2003. Patterns of gamete incompatibility between the blue mussels *Mytilus edulis* and *M. trossulus*. Marine Biology 143:317–325.

Rumrill, S. 1990. Natural mortality of marine invertebrate larvae. Ophelia 32:163–198.

Sewell, M. 1994. Small size, brooding, and protandry in the apodid sea cucumber *Leptosynapta clarki*. Biological Bulletin 187:112–123.

Sewell, M., and D. Manahan. 2001. Echinoderm eggs: biochemistry and larval biology. Pages 55–58 *in* E. Barker, ed. Echinoderms 2000. Routledge, Abingdon.

Shanks, A. 2009. Pelagic larval duration and dispersal distance revisited. Biological Bulletin 216:373–385.

Shropshire, J., B. Leigh, and S. Bordenstein. 2020. Symbiont-mediated cytoplasmic incompatibility: what have we learned in 50 years? eLife 9:e61989.

Skinner, S. 1985. Son-killer: a third extrachromosomal factor affecting the sex-ratio in the parasitoid wasp, *Nasonia* (= *Mormoniella*) *vitripennis*. Genetics 109:745–759.

Smith, C., and S. Fretwell. 1974. The optimal balance between size and number of offspring. American Naturalist 108:499–506.

Soetaert, K., T. Petzoldt, and R. Setzer. 2010. Solving differential equations in R: package deSolve. Journal of Statistical Software 33:1–25.

Stevens, L., R. Giordano, and R. Fialho. 2001. Male-killing, nematode infections, bacteriophage infection, and virulence of cytoplasmic bacteria in the genus *Wolbachia*. Annual Review of Ecology and Systematics 32:519–545.

Strathmann, M. F. 1987. Reproduction and development of marine invertebrates of the northern Pacific coast: data and methods for the study of eggs, embryos, and larvae. University of Washington Press, Seattle.

Strathmann, M. F., and R. R. Strathmann. 2006. A vermetid gastropod with complex intracapsular cannibalism of nurse eggs and sibling larvae and a high potential for invasion. Pacific Science 60:97–108.

Strathmann, R. R. 1978. The evolution and loss of feeding larval stages of marine invertebrates. Evolution 32:894–906.

———. 1985. Feeding and nonfeeding larval development and life-history evolution in marine invertebrates. Annual Review of Ecology and Systematics 16:339–361.

———. 1990. Why life histories evolve different in the sea. American Zoologist 30:197–207.

Styan, C. 1998. Polyspermy, egg size, and the fertilization kinetics of free-spawning marine invertebrates. American Naturalist 152:290–297.

Sunagawa, S., L. Coelho, S. Chaffron, J. Kultima, K. Labadie, G. Salazar, B. Djahanschiri, et al. 2015. Structure and function of the global ocean microbiome. Science 348:1261359.

Thorson, G. 1950. Reproductive and larval ecology of marine bottom invertebrates. Biological Reviews 25:1–45.

Vance, R. 1973. On reproductive strategies in marine benthic invertebrates. American Naturalist 107:339–352.

Warner, R. 1975. The adaptive significance of sequential hermaphroditism in animals. American Naturalist 109:61–82.

Werren, J., L. Baldo, and M. Clark. 2008. *Wolbachia*: master manipulators of invertebrate biology. Nature Reviews Microbiology 6:741–751.

Williams, D., and D. Anderson. 1975. The reproductive system, embryonic development, larval development, and metamorphosis of the sea urchin *Heliocidaris erythrogramma* (Val.) (Echinodea: Echinometridae). Australian Journal of Zoology 23:371–403.

Wray, G. 1996. Parallel evolution of nonfeeding larvae in echinoids. Systematic Biology 45:308–322.

Wray, G., and R. Raff. 1989. Evolutionary modification of cell lineage in the direct-developing sea urchin *Heliocidaris erythrogramma*. Developmental Biology 132:458–470.

———. 1991*a*. The evolution of developmental strategy in marine invertebrates. Trends in Ecology and Evolution 6:45–50.

———. 1991*b*. Rapid evolution of gastrulation mechanisms in a sea urchin with lecithotrophic larvae. Evolution 45:1741–1750.

Young, C., and F.-S. Chia. 1987. Abundance and distribution of pelagic larvae as influenced by predation, behavior, and hydrographic factors. *In* A. Giese, J. Pearse, and V. Pearse, eds. Reproduction of marine invertebrates. Vol. IX. General aspects: seeking unity in diversity. Blackwell Scientific, Palo Alto, CA.

Yund, P. 2000. How severe is sperm limitation in natural populations of marine free-spawners? Trends in Ecology and Evolution 15:10–13.

Zigler, K., E. Raff, E. Popodi, R. Raff, and H. Lessios. 2003. Adaptive evolution of bindin in the genus *Heliocidaris* is correlated with the shift to direct development. Evolution 57:2293–2302.